Research Square

Preprints are preliminary reports that have not undergone peer review.
They should not be considered conclusive, used to inform clinical practice,
or referenced by the media as validated information.

# Comparative Effects of Gaussian, Coloured and State-Dependent Noise on Fractional-Order Chen and Lorenz Chaotic Systems: A Quantitative Analysis Across the Memory-Induced Chaos Boundary

**Iyanuoluwa Olaniyi AJAYI**

ajayi.iyanuoluwa@bouesti.edu.ng

Bamidele Olumilua University of Education, Science and Technology

**Tolulope Ayodeji OJUOLA**

Bamidele Olumilua University of Education, Science and Technology

**Samuel Oyindamola ADEOSUN**

Nigerian Defence Academy

**Samuel Adedapo OLAWOORE**

Ekiti State University

**Research Article**

**Keywords:** fractional-order chaotic systems, Caputo derivative, stochastic Adams-Bashforth-Moulton scheme, Lyapunov exponent, Lorenz and chen system

**Posted Date:** November 18th, 2026

**DOI:** https://doi.org/10.21203/rs.3.rs-11495978/v1

**License:** This work is licensed under a Creative Commons Attribution 4.0 International License.
Read Full License

**Additional Declarations:** No competing interests reported.

# COMPARATIVE EFFECTS OF GAUSSIAN, COLOURED AND STATE-DEPENDENT NOISE ON FRACTIONAL-ORDER CHEN AND LORENZ CHAOTIC SYSTEMS: A QUANTITATIVE ANALYSIS ACROSS THE MEMORY-INDUCED CHAOS BOUNDARY

**Iyanuoluwa Olaniyi AJAYI *(Corresponding Author)*,**
Department of Physics, Bamidele Olumilua University of Education, Science and Technology, P.M.B 250, Ikere Ekiti, Ekiti State, Nigeria

**Email:** ajayiiyanu16@gmail.com, ajayi.iyanuoluwa@bouesti.edu.ng
**ORCID NO.: 0009-0008-6399-0167**

**Tolulope Ayodeji OJUOLA,**
Department of Physics, Bamidele Olumilua University of Education, Science and Technology, P.M.B 250, Ikere Ekiti, Ekiti State, Nigeria

**Email:** ojuola.tolulope@bouesti.edu.ng

**Samuel Oyindamola ADEOSUN,**
Department of Physics, Nigerian Defence Academy, Kaduna, Kaduna State.

**Email:** adeosuns51@gmail.com
**ORCID NO.: 0009-0002-5446-1497**

**Samuel Adedapo OLAWOORE.**
Department of Physics, Ekiti State University, Ado Ekiti, Ekiti State, Nigeria
**Email:** samuelolawoore@gmail.com

## Abstract

*Noise and memory both shape chaotic dynamics, yet the three common noise classes, Gaussian white, temporally correlated and state-dependent, have not been compared on fractional-order chaotic systems under matched intensity conventions. This study compares them on the Caputo fractional-order Lorenz and Chen systems with a stochastic Adams–Bashforth–Moulton scheme in which the noise enters through the memory kernel. The scheme was verified against the exact Mittag-Leffler solution (observed order 1.8–2.0), the exact variance of the stochastic Volterra integral (within 1.3%) and the linear-response theory of the equilibrium fluctuations. The deterministic analysis shows that the classical Lorenz parameters are chaotic only for $q > q = 0.994$, whereas the Chen system is chaotic down to $q = 0.824$, so the fractional order was used relative to this chaos boundary. A full factorial design (two systems, six orders, five noise models, eight intensities, 24 realisations) was analysed with dispersion, attractor deformation, spectral entropy, switching rate and the largest exponent computed along the same noise realisation. Below the boundary, white noise of modest intensity sustains an attractor with a positive exponent ($\lambda_1 = 0.44$ for Lorenz at $q = 0.99$, $\eta = 1$). Above it, strong white noise removes sensitivity to initial conditions in the Chen system ($\lambda_1$ falls from about 2.6 to zero at $\eta = 8$, 12 and 16 for $q = 0.85$, 0.90 and 0.95), although dispersion and switching increase. Coloured noise is weaker than white noise at equal spectral intensity and comparable at equal variance, and state dependence raises the exponent in 43 of 44 significant comparisons and limits survival. Per-step additive noise has no continuum limit, and Box–Muller noise with random arguments is Gaussian noise. These results give a quantitative basis for modelling stochastic fractional-order chaotic systems.*

**Keywords:** fractional-order chaotic systems; Caputo derivative; stochastic Adams-Bashforth-Moulton scheme; Lyapunov exponent; Lorenz and chen system.

## INTRODUCTION

Chaotic systems are deterministic nonlinear systems whose trajectories are bounded, aperiodic and exponentially sensitive to initial conditions (Lorenz, 1963). The Lorenz system and the later Chen system (Chen & Ueta, 1999) have become standard test beds for theory, secure communication, control and circuit design. Real systems are never isolated, however, and noise is unavoidable. Noise can destroy fine attractor structure, but it can also create order: noise-induced order, noise-induced synchronisation and the suppression of period-doubling cascades have all been reported (Crutchfield et al., 1982; Matsumoto & Tsuda, 1983; Gao et al., 1999; Zhou & Kurths, 2002). Which of these outcomes occurs depends on how the noise is correlated in time and on how its amplitude relates to the state of the system, so the statistical nature of the noise must be treated as a control variable rather than a detail.

A second ingredient is memory. Fractional calculus replaces the integer-order derivative by a convolution with a power-law kernel, so that the present rate of change depends on the whole history of the state (Podlubny, 1999; Kilbas et al., 2006). Fractional-order versions of the Lorenz and Chen systems keep chaotic attractors, but only inside a limited range of orders (Grigorenko & Grigorenko, 2003; Ahmad & Sprott, 2003; Li & Peng, 2004; Lu & Chen, 2006). The reason is structural. For a Caputo system of order $q$, an equilibrium is stable when every eigenvalue $\lambda$ of its Jacobian satisfies $|\arg\lambda| > q\pi/2$ (Matignon, 1996), and a double-scroll attractor needs unstable saddle-focus equilibria (Tavazoei & Haeri, 2007). Lowering $q$ therefore moves the system towards the boundary where the equilibria become stable and chaos is lost. This chaos boundary is a property of the memory, and it can be computed exactly for each system.

Several authors have combined noise with fractional-order chaotic systems. Adelakun et al. (2019) added a Box–Muller-type function of the state variables to one equation of the fractional Chen and Arneodo-Coullet systems and reported that it narrows the period-doubling windows. Das et al. (2016), Almutairi and Saber (2024) and He et al. (2018) studied random switching of parameters or orders in fractional Lorenz-family systems. On the numerical side, Euler-Maruyama schemes have been developed for stochastic Volterra and Caputo stochastic differential equations (Zhang, 2008; Doan et al., 2020). These research shows that noise matters for fractional chaos, but they leave four gaps open. (a) No study compares white Gaussian, temporally correlated (coloured) and state-dependent forcing on the fractional Lorenz and Chen systems under explicitly matched intensity conventions. Without matching, differences between noise types cannot be separated from differences in forcing strength. (b) The fractional order has been treated as one more parameter. Its position relative to the chaos boundary of Matignon's criterion has not been used to organise the noise response, although the deterministic dynamics on the two sides of this boundary (chaos versus a stable equilibrium) are qualitatively different. (c) Stochastic forcing is often added to the state after each step. That update has no memory kernel and is not a discretisation of a stochastic Caputo equation. A stochastic Adams-Bashforth-Moulton scheme whose noise enters through the same Volterra kernel as the drift, and whose noise statistics are verified against exact results, has not been used for such comparisons. (d) Claims that noise ‘suppresses’ or ‘preserves’ chaos have usually rested on phase portraits. A quantitative criterion is needed, namely the largest

Lyapunov exponent of the noisy system computed along the same noise realisation, supported by deformation, spectral and switching statistics with uncertainty estimates.

Hypothesis. Because the stability boundary is set by the memory, the response to noise should depend on which side of it the system lies. Below the boundary the equilibria are stable and noise should produce irregular excursions whose size grows with noise intensity and depends on the noise spectrum through the linear response of the equilibrium. Above the boundary the attractor already exists, and noise should deform it and change its spectral and switching statistics, while the sign of the largest Lyapunov exponent is expected to be much harder to change.

The research aim to determine, by controlled and verified simulation, how Gaussian white noise, coloured (Ornstein–Uhlenbeck) noise and state-dependent noise act on the Caputo fractional-order Lorenz and Chen systems, and how that action depends on the fractional order relative to the chaos boundary of each system. The specific objectives are to; derives and verifies a stochastic Adams–Bashforth–Moulton scheme in Volterra form, and checks its drift order, noise variance, multiplicative-noise moments and tangent dynamics against exact results; characterises the deterministic reference dynamics of both systems versus fractional order, including the exact chaos boundary, the largest Lyapunov exponent and the 0–1 test; defines white, coloured and state-dependent noise with matched intensity conventions, and compares them with quantitative diagnostics (deformation, spectral entropy, correlation time, switching rate and Lyapunov exponent) over a range of fractional orders and intensities, with repeated realisations; tests the effect of the noise correlation time under two matching rules (equal spectral intensity and equal variance); ests the numerical robustness of the conclusions against the time step and shows why per-step additive noise is not a valid fractional noise model; and to states explicit operational criteria under which noise can be said to suppress or preserve chaos.

The four questions of the original study are made testable: (RQ1) what does Gaussian noise do to the fractional systems on each side of the chaos boundary? (RQ2) how does state-dependent amplitude change this compared with additive noise? (RQ3) which noise type is most effective at removing chaos, judged by the Lyapunov exponent along a common noise realisation? (RQ4) how does fractional memory, measured by the distance of $q$ from the chaos boundary, change the noise-induced behaviour?

The contribution of this research are as follow (i) A single, reproducible framework in which three noise classes enter the Caputo systems through the same memory kernel with matched intensities. (ii) The exact chaos boundary of both systems is used as the organising variable, which exposes that the fractional Lorenz system is chaotic only for $q \gtrsim 0.994$ whereas the Chen system stays chaotic down to $q \approx 0.824$. (iii) Quantitative, uncertainty-aware comparison of the noise types, including the effect of the correlation time. (iv) Verified numerics and explicit failure analysis of per-step additive noise. The memory-based diagnostics follow the validated-spectrum protocol of Ajayi (2026), who analysed a six-dimensional series memcapacitor oscillator whose internal memory variables also make the dynamics history dependent (Adelakun et al., 2026). The present study carries that protocol, with positive-exponent thresholds, step-size sensitivity and time-convergence of exponents, from deterministic memory circuits to noisy fractional-order systems.

## METHODOLOGY

### Fractional-Order Chen and Lorenz Systems

Memory is introduced through the Caputo derivative. For $0 < q \leq 1$ and a differentiable function $f(t)$,

$$ {}^{C}D_t^q f(t) = \frac{1}{\Gamma(1-q)} \int_0^t (t-s)^{-q} f'(s)\, ds, \tag{1} $$

where $\Gamma(\cdot)$ is the Gamma function. The Caputo form is used because it accepts the classical initial conditions $x(0), y(0), z(0)$. With the state vector $X = (x, y, z)^{\mathsf{T}}$, the fractional Lorenz system is

$$ \begin{aligned} {}^{C}D_t^q x &= \sigma(y - x), \\ {}^{C}D_t^q y &= rx - y - xz, \\ {}^{C}D_t^q z &= xy - bz, \end{aligned} \tag{2} $$

and the fractional Chen system is

$$ \begin{aligned} {}^{C}D_t^q x &= a(y - x), \\ {}^{C}D_t^q y &= (c - a)x - xz + cy, \\ {}^{C}D_t^q z &= xy - bz. \end{aligned} \tag{3} $$

Both are written compactly as ${}^{C}D_t^q X = F(X)$. The parameters are $(\sigma, r, b) = (10, 28, 8/3)$ for Equ. (2) and $(a, b, c) = (35, 3, 28)$ for Equ. (3), the values at which the integer-order systems are chaotic. The initial condition is $X(0) = (0.1, 0.1, 0.1)^{\mathsf{T}}$ throughout, except where stated. A parameter set that is chaotic at $q = 1$ is not necessarily chaotic at $q < 1$, so the deterministic fractional systems are analysed first.

### Equilibria and the Chaos Boundary

The nonzero equilibria are

$$ \begin{aligned} E_L^{\pm} &= \left(\pm\sqrt{b(r-1)},\ \pm\sqrt{b(r-1)},\ r-1\right), \\ E_C^{\pm} &= \left(\pm\sqrt{b(2c-a)},\ \pm\sqrt{b(2c-a)},\ 2c-a\right). \end{aligned} \tag{4} $$

Matignon's criterion states that the linearisation about an equilibrium is asymptotically stable when all Jacobian eigenvalues $\lambda_i$ obey

$$ |\arg\lambda_i| > \frac{q\pi}{2}. \tag{5} $$

At $E_L^{\pm}$ the Jacobian has one negative real eigenvalue ($-13.855$) and a complex pair $0.0940 \pm 10.1945\,\mathrm{i}$. At $E_C^{\pm}$ it has $-18.428$ and $4.2140 \pm 14.8846\,\mathrm{i}$. For the complex pair the equilibrium loses stability when $q$ exceeds the critical order

$$ q^* = \frac{2}{\pi} |\arg\lambda_c|, \tag{6} $$

which gives $q_L^* = 0.99413$ and $q_C^* = 0.82436$. Below $q^*$ the saddle-focus equilibria are stable, a necessary condition for the double-scroll attractor is violated and the deterministic system relaxes to an equilibrium.

**Noise Models**

Stochastic forcing is added to every state equation. To keep the equation actually solved explicit, the stochastic fractional system is defined through its Volterra form, which is equivalent to the Caputo initial-value problem:

$$X(t) = X(0) + \frac{1}{\Gamma(q)} \int_0^t (t-s)^{q-1} F\big(X(s)\big)\, ds + \frac{1}{\Gamma(q)} \int_0^t (t-s)^{q-1}\, \Phi(s)\, ds. \tag{7}$$

The forcing term $\Phi$ is, for white noise, the formal derivative of a Wiener process multiplied by an amplitude, and for coloured noise a continuous random process. Four forcing laws are used. All have the same dimension, so their intensity $\eta$ is expressed in the same units (state units per unit time$^{1/2}$).

**Gaussian white noise (W).** The forcing is additive and delta-correlated,

$$\Phi_i(t) = \eta\, \xi_i(t), \qquad \langle \xi_i(t) \rangle = 0, \quad \langle \xi_i(t) \xi_j(s) \rangle = \delta_{ij}\, \delta(t-s), \tag{8}$$

with independent components. The integral in Equ. (7) is then a stochastic Volterra integral with respect to Wiener increments $\mathrm{d}W_i$, interpreted in the Itô sense.

**Coloured noise.** The forcing is an Ornstein–Uhlenbeck process (Uhlenbeck & Ornstein, 1930), generated by

$$\Phi_i(t) = A\, \zeta_i(t), \qquad \mathrm{d}\zeta_i = -\frac{\zeta_i}{\tau}\, \mathrm{d}t + \sqrt{\frac{2}{\tau}}\, \mathrm{d}W_i, \qquad A = \frac{\eta}{\sqrt{2\tau}}, \tag{9}$$

where $\tau > 0$ is the correlation time and $\zeta_i$ is started from its stationary distribution. Its autocovariance and power spectral density are

$$C_\Phi(s) = \frac{\eta^2}{2\tau}\, e^{-|s|/\tau}, \qquad S_\Phi(\omega) = \frac{\eta^2}{1 + \omega^2 \tau^2}. \tag{10}$$

The choice of $A$ in Equ. (9) fixes the spectral density at zero frequency to $\eta^2$, the same as for white noise. This is the usual convention for comparing coloured and white noise at equal intensity (Hänggi & Jung, 1995). As $\tau \to 0$ the OU forcing converges to the white forcing of Equ. (8). A second, variance-matched convention, $A = \eta$, fixes the stationary standard deviation instead; both are tested.

**State-dependent noise (SW and SOU).** In the state-dependent models the amplitude is modulated by the instantaneous distance of the state from the origin,

$$g(X) = \frac{\| X \|}{R_N}, \qquad \Phi_i(t) = g\big(X(t)\big)\, \Phi_i^{(\mathrm{W\ or\ OU})}(t), \tag{11}$$

where $R_N = 27.8$ is the root-mean-square norm of the integer-order attractors (27.82 for Lorenz, 27.73 for Chen). The normalisation makes the mean-square modulation close to one on the attractor, $\langle g^2 \rangle \approx 1$, so a state-dependent run at intensity $\eta$ is compared with an additive run at the same $\eta$ on a like-for-like basis; the realised $\langle g^2 \rangle$ is reported for every run. The modulation is multiplicative: large excursions receive larger kicks and the state near the origin is almost unperturbed. SW denotes white and SOU denotes OU noise with this modulation. Table 1 summarises the models.

**Table 1.** Noise models compared in this study. All components are driven by independent noise sources.

| Label | Forcing $\Phi_i(t)$ | Correlation | State dependence | Matching rule |
|---|---|---|---|---|
| W | $\eta\,\xi_i(t)$ | none (white) | none (additive) | spectral intensity $\eta^2$ |
| OU | $\frac{\eta}{\sqrt{2\tau}}\zeta_i(t)$ | exponential, time $\tau$ | none (additive) | spectral intensity $\eta^2$ |
| OU-V | $\eta\,\zeta_i(t)$ | exponential, time $\tau$ | none (additive) | stationary variance $\eta^2$ |
| SW | $\eta\,g(X)\,\xi_i(t)$ | none (white) | multiplicative, $g = \| X \| / R_N$ | $\langle g^2 \rangle \approx 1$ |
| SOU | $\frac{\eta}{\sqrt{2\tau}}\,g(X)\,\zeta_i(t)$ | exponential, time $\tau$ | multiplicative, $g = \| X \| / R_N$ | $\langle g^2 \rangle \approx 1$ |

**A note on Box–Muller noise.** The Box–Muller transform converts two independent uniform variables $U_1, U_2 \in (0,1)$ into a Gaussian variable, $d\sqrt{-2\ln U_1}\cos(2\pi U_2)$. If $U_1, U_2$ are random it produces exactly Gaussian noise, so it cannot define a distinct, state-dependent noise. In Adelakun et al. (2019) the arguments are the state variables themselves, so the term is a deterministic nonlinear feedback, not a random process. The state dependence in the present study is therefore defined explicitly by Equ. (11).

**Stochastic Adams–Bashforth–Moulton Scheme**

Let $t_n = nh$ and $X_n \approx X(t_n)$. The deterministic part follows the fractional Adams–Bashforth–Moulton predictor–corrector method of Diethelm et al. (2002), whose convergence order is $\min(2, 1+q)$ (Diethelm et al., 2004), and the noise enters through the same Volterra kernel. Writing $F_j = F\big(X_j\big) + \Phi_j^{\mathrm{ou}}$ for the drift (including any coloured forcing) and $\Theta_j = \eta\, g\big(X_j\big)\,\xi_j$ for the white forcing amplitude at node $j$, the predictor is

$$X_{n+1}^{P} = X_0 + \frac{h^q}{\Gamma(q+1)} \sum_{j=0}^{n} b_{n-j}\, F_j + \sum_{j=0}^{n} \omega_{n+1-j}\, \Theta_j, \tag{12}$$

and the corrector is

$$X_{n+1} = X_0 + \frac{h^q}{\Gamma(q+2)} \left[ F(X_{n+1}^{P}) + \alpha_n F_0 + \sum_{j=1}^{n} a_{n-j}\, F_j \right] + \sum_{j=0}^{n} \omega_{n+1-j}\, \Theta_j, \tag{13}$$

with the drift weights

$$\begin{aligned} b_m &= (m+1)^q - m^q, \qquad a_m \\ &= (m+2)^{q+1} + m^{q+1} - 2(m+1)^{q+1}, \\ \alpha_n &= n^{q+1} - (n-q)(n+1)^q. \end{aligned} \tag{14}$$

The noise weights follow from the exact variance of the Volterra kernel over one step, so that the variance of the discretised stochastic convolution matches the continuous one:

$$\omega_m = \frac{1}{\Gamma(q)}\sqrt{\frac{h^{2q-1}[m^{2q-1} - (m-1)^{2q-1}]}{2q-1}}, \qquad \xi_j \sim \mathcal{N}(0,1) \text{ i. i. d.} \tag{15}$$

For $q = 1$ one has $\omega_m = \sqrt{h}$ and the scheme reduces to the Heun–Euler–Maruyama method. The history terms are retained in full, so the memory is never truncated. The OU process is advanced with its exact one-step transition,

$$\zeta_{n+1} = e^{-h/\tau}\zeta_n + \sqrt{1 - e^{-2h/\tau}}\ \nu_n, \qquad \nu_n \sim \mathcal{N}(0,1), \tag{16}$$

so that the forcing is statistically exact at every step size. The step is $h = 0.01$ unless stated, and $T = 150$ time units with the first $T_{tr} = 30$ discarded as transient.

**Lyapunov Exponent of the Noisy Fractional System**

For a Caputo system the solution depends differentiably on the initial condition, so a perturbation $\delta(t)$ obeys the variational equation obtained by differentiating Equ. (7) along the same noise realisation,

$${}^{C}D_t^q \delta = J\big(X(t)\big)\delta + [\nabla g \cdot \delta]\Phi^{(0)}(t), \tag{17}$$

where $J$ is the Jacobian of $F$ and the last term is present only for state-dependent noise ($\Phi^{(0)}$ is the unmodulated forcing). Because the equation is linear in $\delta$, the whole stored history of $\delta$ can be rescaled by the same factor as $\delta$ itself, which is the fractional equivalent of Benettin renormalisation (Danca & Kuznetsov, 2018, use a related Benettin-type procedure for fractional systems). The largest exponent is

$$\lambda_1 = \lim_{T\to\infty}\frac{1}{T}\sum_k \ln s_k, \qquad s_k = \frac{\| \delta(t_k^-) \|}{\| \delta(t_{k-1}^+) \|}, \tag{18}$$

with rescaling every 0.5 time units. Because $\delta$ evolves along the same noise realisation as $X$, $\lambda_1$ measures sensitivity to the initial condition for a given forcing record, the quantity that decides whether noise has produced order in the random-dynamical-systems sense (Arnold, 1998). A negative value means that nearby trajectories driven by the same noise converge; a positive value means they separate. For stable regimes the Caputo response decays algebraically, so $\lambda_1$ is small and negative. A threshold $|\lambda_1| < 0.05$ is treated as neutral, following the threshold-based classification of Ajayi (2026). As an independent check, twin trajectories separated by $10^{-8}$ and driven by the same noise are also integrated.

**Diagnostics**

All diagnostics use the retained part of each trajectory, $t > T_{tr}$.

1. Dispersion: the mean of the standard deviations of $x, y, z$, $S_{tot}$.

Attractor deformation: the mean distance of the noisy trajectory from the deterministic attractor of the same order $q$ (a long reference orbit), $D_{def} = \langle \min_{y\in\mathcal{A}_q} \| X(t) - y \| \rangle_t$, computed with a k-d tree. A noise-free run gives $D_{def} \approx 0$.

2. Correlation time $\tau_{ac}$: the lag at which the autocorrelation of $x$ first falls below $1/e$.
3. Normalised spectral entropy of $x$, from Welch's periodogram (Welch, 1967): $H = -\sum p_k \ln p_k / \ln K$ with $p_k$ the fraction of power in bin $k$. $H$ is near 0 for a line spectrum and near 1 for a flat spectrum.

4. Switching rate $\nu$: the number of transitions of $x$ between $x > 3$ and $x < -3$ per unit time, which counts passages between the two lobes of the attractor.
5. Survival: the fraction of runs that remain bounded ($|X| < 10^7$).

For the equilibrium regime the linear response gives a closed-form prediction that serves as a check on the whole simulation chain. Linearising about a stable equilibrium with additive forcing of spectral density $S_\Phi(\omega)$, the stationary variance of component $i$ is

$$\mathrm{Var}(x_i) = \frac{1}{\pi}\int_0^\infty \sum_j \left|H_{ij}(\omega)\right|^2 S_\Phi(\omega)\, d\omega, \qquad H(\omega) = [(\mathrm{i}\omega)^q I - J]^{-1}, \quad (19)$$

evaluated by numerical quadrature and compared with the simulations.

The main experiment is a full factorial design: system (Lorenz, Chen) × fractional order $q$ (0.95, 0.99, 0.995, 1.0 for Lorenz and 0.80, 0.85, 0.90, 0.95, 0.99, 1.0 for Chen, chosen on both sides of the chaos boundary) × noise model (W, OU, SW, SOU, OU-V) × intensity $\eta \in \{0.5,1,2,4,6,8,12,16\}$ × 24 independent noise realisations, plus 24 noise-free runs with perturbed initial conditions per $q$. The correlation time is $\tau = 0.5$. A separate sweep varies $\tau$ over 0.05–5 at $\eta = 8$ under the equal-intensity rule. Step-size tests use $h = 0.02,0.01,0.005$ with common random numbers obtained by coarse-graining the finest noise path. Results are reported as mean $\pm$ 95% confidence interval over realisations. Noise types are compared with the Kruskal–Wallis test and pairwise Mann–Whitney tests with Holm correction (Holm, 1979), and effect sizes are reported as differences of medians. Chaos classification uses the 0–1 test of Gottwald and Melbourne (2004, 2009) together with $\lambda_1$.

## RESULTS AND DISCUSSIONS

### Verification of the Numerical Scheme

Before any noise comparison, the scheme was tested against exact results. (i) *Drift convergence.* For the linear test problem ${}^C D_t^q y = -y$, $y(0) = 1$, the error against the exact Mittag-Leffler solution decreases with the observed orders 1.80, 1.90 and 2.01 for $q = 0.8$, 0.9 and 1.0, in agreement with the theoretical order $\min(2, 1+q)$ of the Adams method (Fig. 1a). (ii) *Noise variance.* For zero drift, the variance of the discretised stochastic Volterra integral agrees with the exact value $\eta^2 t^{2q-1}/[\Gamma(q)^2(2q-1)]$ to within 0.4% (Monte-Carlo ratio 0.996 to 0.997 over $q = 0.8$, 0.9, 1; Fig. 1b). With a linear drift the agreement is within 1.3%, and the variance of integrated OU forcing at $q = 1$ is 10.06 against the exact 10.13. (iii) *Tangent equation.* The solution of the variational equation agrees with central finite differences of two trajectories driven by the same noise to a relative error below $7 \times 10^{-5}$ for all five forcing models and both systems. (iv) *Box–Muller.* A Kolmogorov–Smirnov test on $2 \times 10^5$ values of $d\sqrt{-2\ln U_1}\cos(2\pi U_2)$ with independent uniform $U_1, U_2$ cannot distinguish them from $\mathcal{N}(0, d^2)$ (D = 0.0024, p = 0.20; skewness and excess kurtosis are 0.00 and 0.01). This confirms that the Box–Muller construction in the original manuscript is Gaussian noise and not a separate noise class.

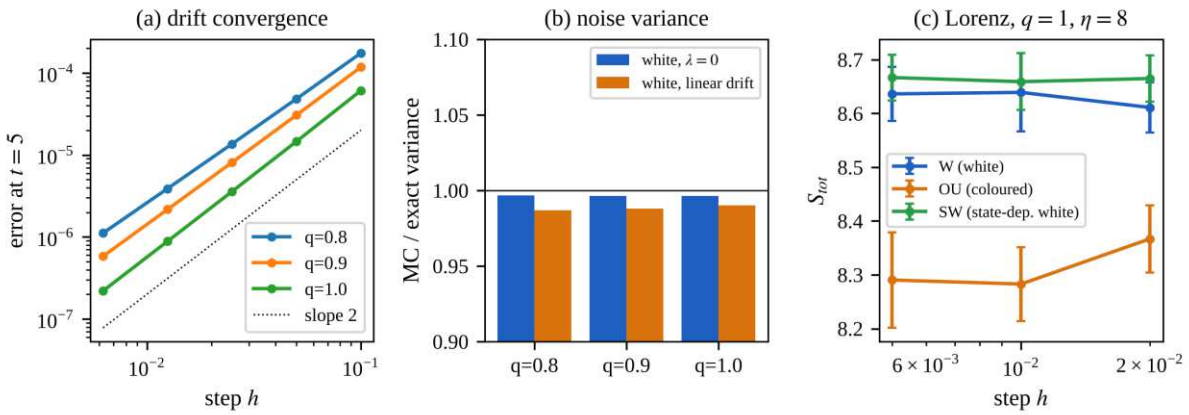



**Figure 1.** Verification of the stochastic scheme. (a) Error of the drift discretisation for the linear test problem against the exact Mittag-Leffler solution, with the slope-2 reference. (b) Ratio of the Monte-Carlo to the exact variance of the stochastic Volterra integral for zero drift and for linear drift. (c) Dispersion $S_{tot}$ of the Lorenz system at $q = 1, \eta = 8$ as a function of the step $h$, with 95% confidence intervals over 16 realisations driven by common random numbers.

**Deterministic Reference Dynamics and the Chaos Boundary**

**Table 2.** Deterministic reference dynamics of the fractional Lorenz and Chen systems. The equilibria are unstable in the sense of Equ. (5) when $q > q^*$ ($q_L^* = 0.99413$, $q_C^* = 0.82436$).

| **System** | $q$ | **Saddle-focus equilibria** | **std of $x$ (late)** | **$\lambda_1$ (mean ± sd over 4 initial conditions)** | **0–1 test $K$** | **Classification** |
|---|---|---|---|---|---|---|
| Lorenz | 0.90 | stable | 0.001 | -0.007 ± 0.000 | -0.53 | stable equilibrium |
| Lorenz | 0.95 | stable | 0.000 | -0.006 ± 0.000 | -0.53 | stable equilibrium |
| Lorenz | 0.99 | stable | 0.005 | -0.030 ± 0.001 | -0.05 | stable equilibrium |
| Lorenz | 0.995 | unstable | 7.883 | 0.881 ± 0.019 | 1.00 | chaotic |
| Lorenz | 1.00 | unstable | 7.927 | 0.902 ± 0.010 | 1.00 | chaotic |
| Chen | 0.80 | stable | 0.002 | -0.005 ± 0.000 | -0.53 | stable equilibrium |
| Chen | 0.85 | unstable | 7.580 | 2.562 ± 0.023 | 1.00 | chaotic |
| Chen | 0.90 | unstable | 7.770 | 2.298 ± 0.177 | 1.00 | chaotic |
| Chen | 0.95 | unstable | 8.031 | 2.631 ± 0.018 | 1.00 | chaotic |
| Chen | 0.99 | unstable | 7.162 | -0.001 ± 0.003 | -0.00 | periodic |
| Chen | 1.00 | unstable | 8.465 | 2.070 ± 0.126 | 1.00 | chaotic |

Table 2 and Figure 2 give the deterministic reference. The Lorenz system relaxes to a stable equilibrium for every order $q \leq 0.99$ that was tested and becomes chaotic abruptly at $q_L^* = 0.994$: the exponent $\lambda_1$ jumps from $-0.02$ at $q = 0.993$ to $+0.87$ at $q = 0.995$ (fine sweep in Fig. 2a). Just below the boundary the relaxation is so slow

that a finite run still shows transient chaos ($\lambda_1 = 0.20$ at $q = 0.9935, T = 150$). The same parameter set that is chaotic at $q = 1$ is therefore not chaotic in the fractional Lorenz system for $q \lesssim 0.994$, a fact that the original study did not examine. This is a direct consequence of Equ. (5): the complex pair $0.094 \pm 10.19\,\mathrm{i}$ lies only 0.5% inside the stability region at $q = 1$, so any memory restabilises it. The Chen system stays chaotic over a much wider range, $0.82 \leq q \leq 1$, with $\lambda_1 \approx 2{-}2.7$ and $K = 1.00$. It collapses to an equilibrium for $q \leq 0.815$; at $q = 0.815$ the chaos is transient (the run is still chaotic at $T = 150$ but has settled at $T = 600$), and between 0.82 and $q_C^* = 0.824$ a chaotic attractor coexists with the stable equilibria, so the boundary of Equ. (6) is exact for the equilibria and a close guide, not a strict limit, for the attractor. Inside this range it has narrow periodic windows (for example near $q = 0.94$ and $q = 0.99$, where $\lambda_1 \approx 0$ and $K \approx 0$; Fig. 2b), which will matter for the noise response. Between the boundary and $q = 1$ the exponent is not monotonic in $q$, so the fractional order is not a simple measure of chaoticity.

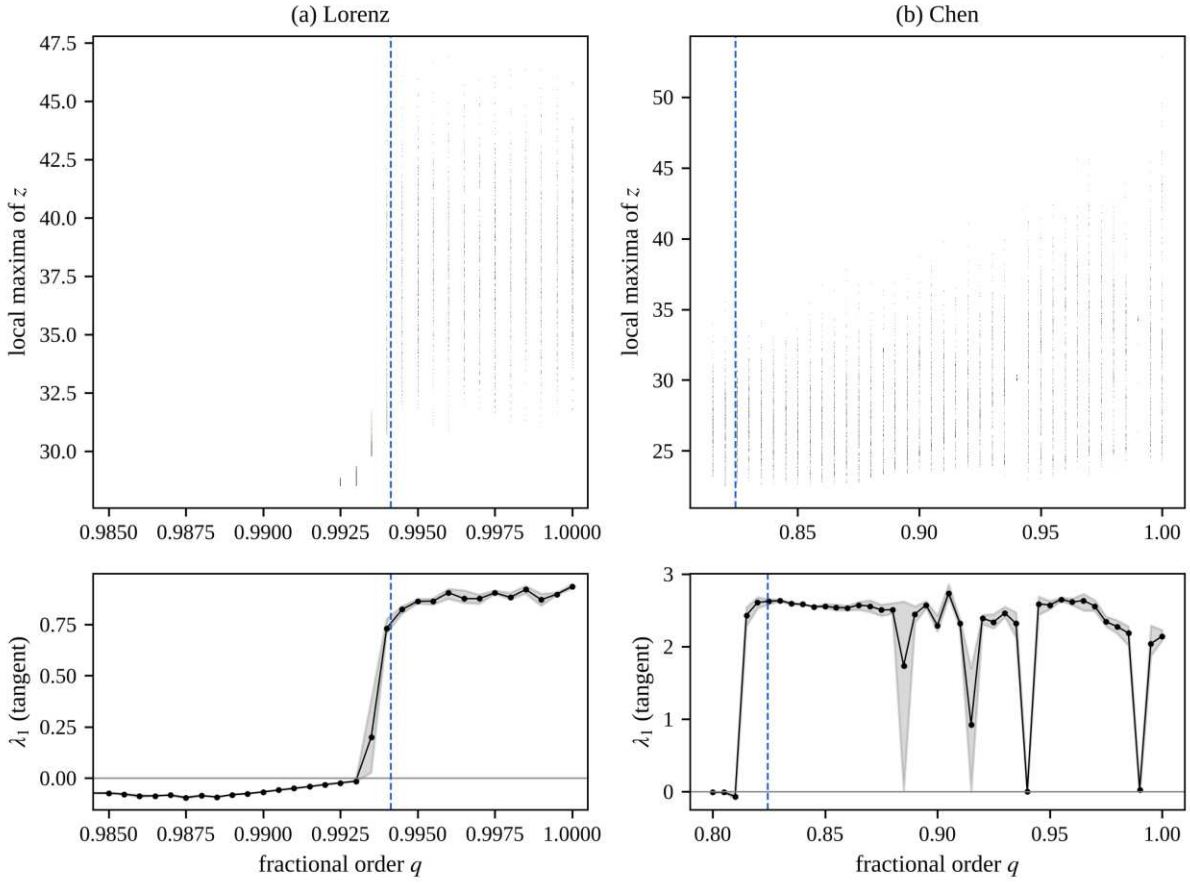



**Figure 2.** Deterministic dynamics against fractional order. Top: local maxima of $z$ (three initial conditions per $q$). Bottom: largest exponent $\lambda_1$ from the tangent equation (line: mean, band: range). The dashed line marks the critical order $q^*$ from Equ. (6). (a) Lorenz, fine sweep $0.985 \leq q \leq 1$. (b) Chen.

The stable regime deserves a comment on the exponent. For $q < q^*$ the deterministic relaxation of a Caputo system is algebraic and not exponential, so $\lambda_1$, defined as the slope of $\ln \| \delta \|$, is small and negative (about $-0.006$ at $q = 0.9$) rather than strongly negative. This is why the classification uses a neutral band $|\lambda_1| < 0.05$ together with the late-time standard deviation.

### Equilibrium Regime: Linear-Response Prediction

Below the chaos boundary the noise acts on a stable equilibrium, and for weak noise the response can be computed. Equ. (19) gives the stationary standard deviation of each component. Figure 3 compares it with the simulations. For Lorenz at $q = 0.95$ the ratio of simulated to predicted standard deviation is 0.991–0.999 for white noise and 0.980–1.000 for OU noise over $\eta = 0.5$–2, which is the accuracy of a 24-realisation estimate. Closer to the boundary, at $q = 0.99$, the OU response still follows the prediction (ratio 1.02–1.04 at $\eta \leq 1$), whereas the white-noise response exceeds it already at $\eta = 0.5$ (ratio about 1.50), because the large variance predicted by the theory (the equilibrium is only weakly damped) drives the trajectory into the nonlinear region. This agreement validates the full chain, from the Volterra weights to the noise generators, with an independent analytic result, and it shows where linear theory stops being valid.

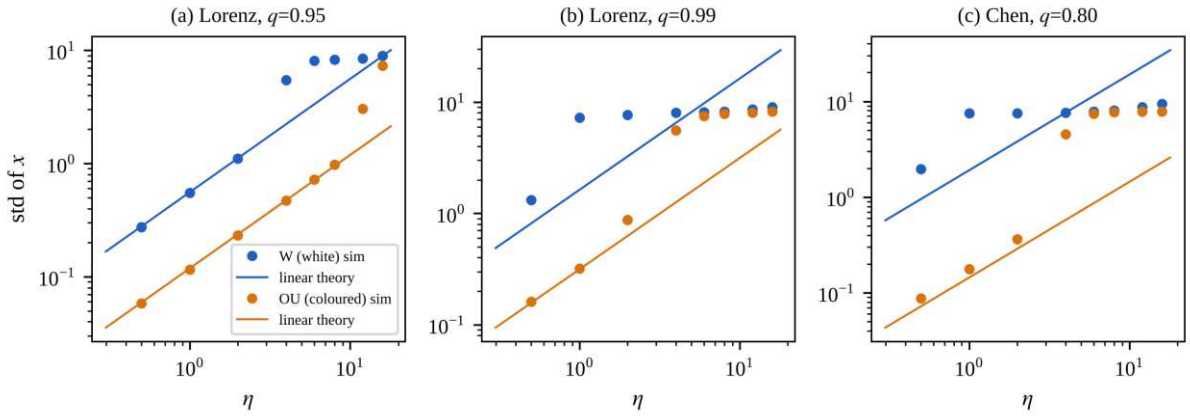



**Figure 3.** Standard deviation of $x$ around a stable equilibrium against noise intensity: simulations (symbols) and the linear-response prediction of Equ. (19) (lines), for white noise and for OU noise with $\tau = 0.5$. (a) Lorenz, $q = 0.95$. (b) Lorenz, $q = 0.99$, close to the boundary, where the white-noise response leaves the linear regime. (c) Chen, $q = 0.80$.

### Effect of the Noise Type: Geometry, Time Series and Spectrum

Figures 4 and 5 show the $(x, z)$ projections at $\eta = 8$ and $\tau = 0.5$ for orders below, near and above the boundary. These pictures are qualitative; the quantitative comparison follows in Table 3. For Lorenz at $q = 0.95$ and 0.99 the deterministic motion is a point, yet white and state-dependent noise generate a broad, butterfly-shaped cloud, while OU noise at the same spectral intensity produces a small blob at $q = 0.95$ and, at $q = 0.99$, a thin and well-organised butterfly with clear spiral lobes. At $q = 1$ all three noises leave the butterfly recognisable, white and state-dependent noise thicken it and OU noise barely changes it. The Chen portraits (Fig. 5) show the same ordering. Figure 6 shows the corresponding time series: the equilibrium regime acquires irregular oscillations whose envelope depends on the noise type. These traces illustrate why a time series that looks irregular cannot by itself indicate chaos: irregular behaviour in the equilibrium regime is entirely noise driven.

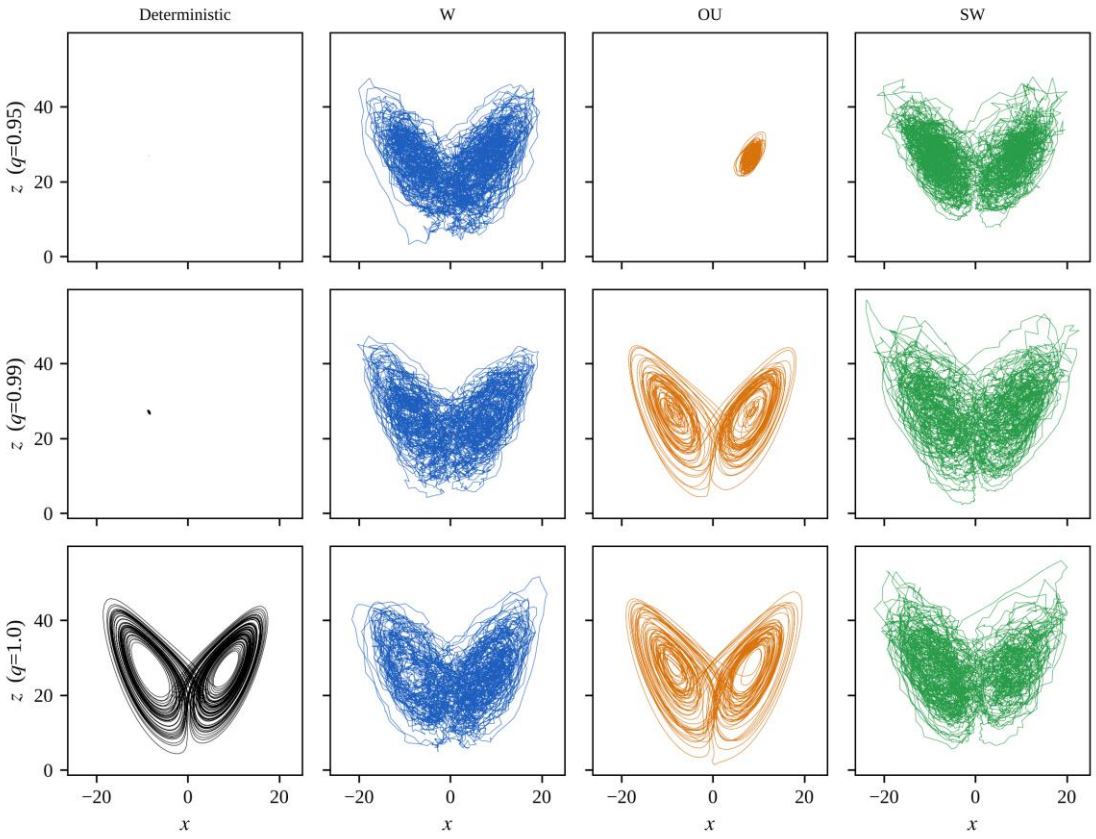



**Figure 4.** Phase portraits $(x, z)$ of the fractional Lorenz system at $\eta = 8$, $\tau = 0.5$ (one realisation, $t > 30$). Rows: $q = 0.95$, 0.99 (below the boundary) and 1.0 (above). Columns: deterministic, white (W), OU, state-dependent white (SW).

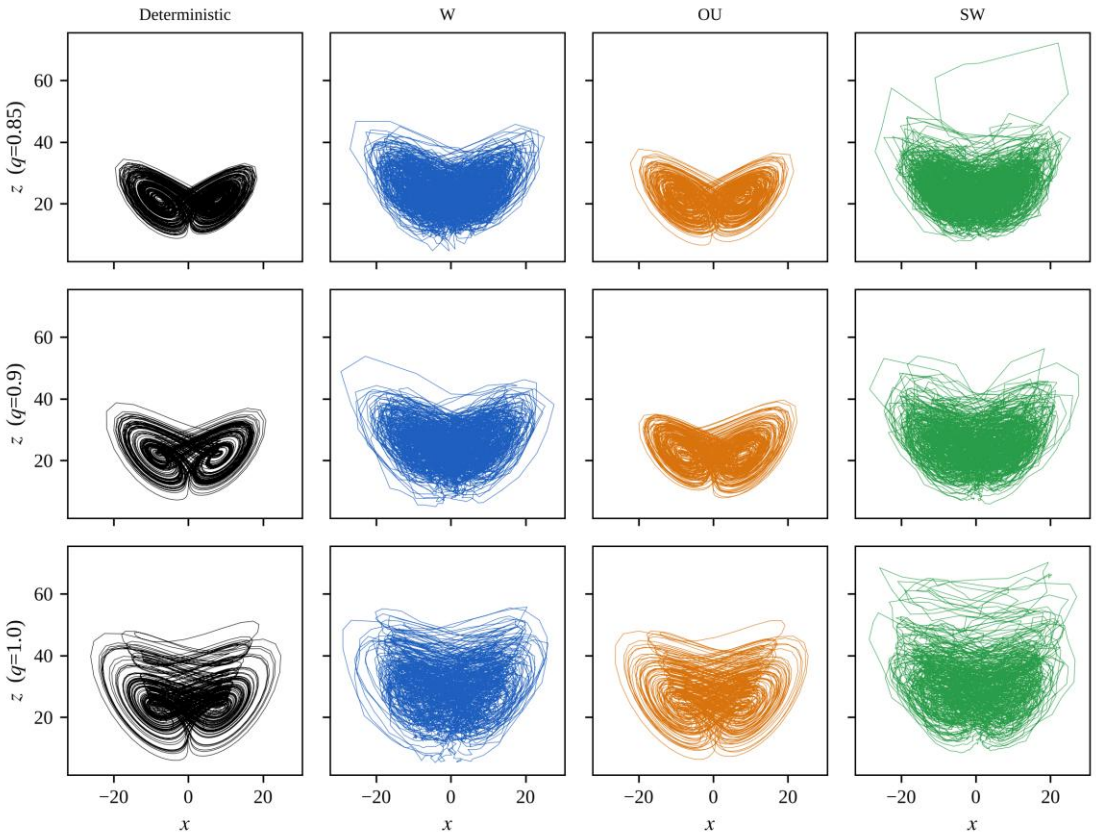



**Figure 5.** Phase portraits $(x, z)$ of the fractional Chen system at $\eta = 8$, $\tau = 0.5$. Rows: $q = 0.85$, 0.90, 1.0. Columns as in Fig. 4.

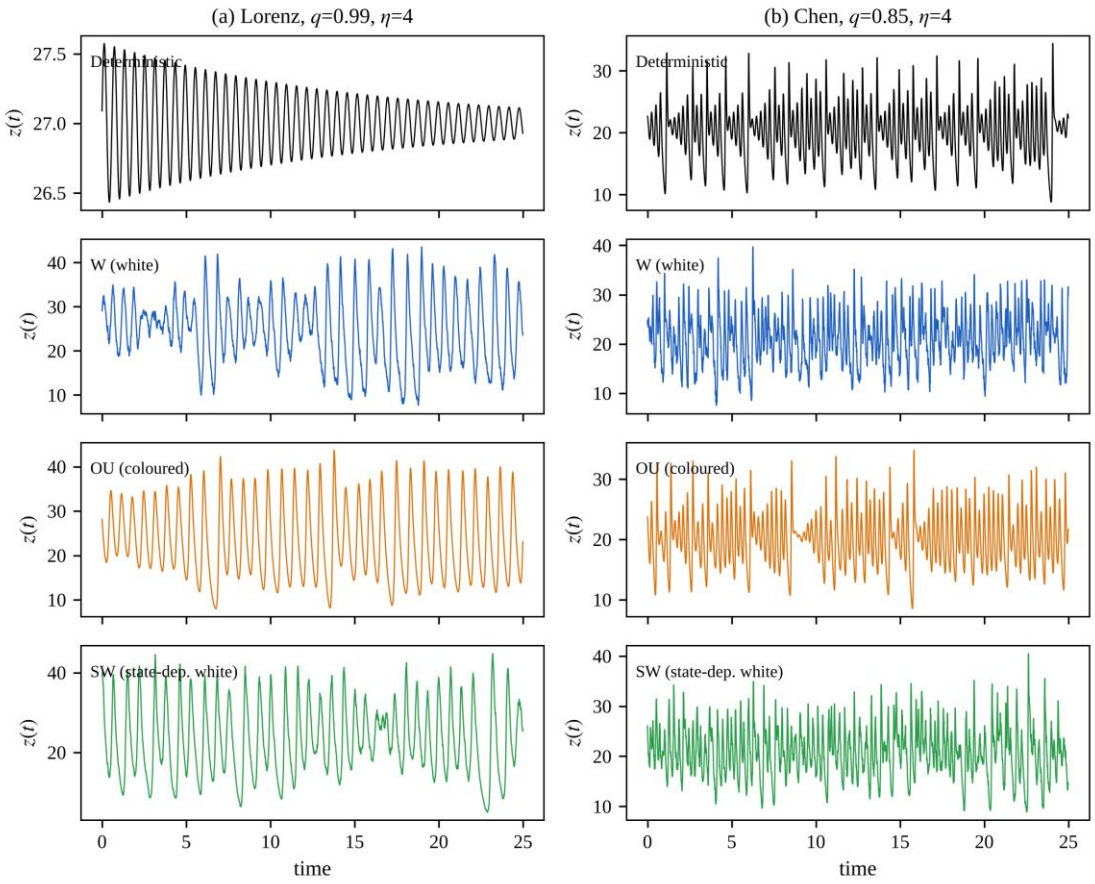



**Figure 6.** Time series $z(t)$ at $\eta = 4$, $\tau = 0.5$ for (a) Lorenz at $q = 0.99$ (equilibrium regime) and (b) Chen at $q = 0.85$ (chaotic regime). Rows: deterministic, W, OU, SW.

**Table 3.** Response at $\eta = 8$ (OU and SOU with $\tau = 0.5$): mean ± 95% confidence interval over 24 realisations. $S_{tot}$ : dispersion; $D_{def}$ : deformation from the deterministic attractor; $\nu$ : switching rate; $\lambda_1$ : tangent exponent along the noise realisation; Survival: fraction of bounded runs. The deterministic rows use 24 perturbed initial conditions.

| **System** | $q$ | **Noise** | $S_{tot}$ | $D_{def}$ | $\nu$ | $\lambda_1$ | **Survival** |
|---|---|---|---|---|---|---|---|
| Lorenz | 0.99 | — | 0.08 ± 0.00 | 12.03 ± 4.89 | 0.00 ± 0.00 | -0.07 ± 0.00 | 100% |
| | | W | 8.51 ± 0.03 | 17.14 ± 0.32 | 0.60 ± 0.02 | 0.72 ± 0.04 | 100% |
| | | OU | 7.79 ± 0.15 | 17.62 ± 0.89 | 0.25 ± 0.03 | 0.43 ± 0.04 | 100% |
| | | SW | 8.60 ± 0.03 | 17.27 ± 0.22 | 0.59 ± 0.01 | 0.91 ± 0.05 | 100% |
| | | SOU | 7.70 ± 0.14 | 16.18 ± 1.34 | 0.25 ± 0.03 | 0.45 ± 0.04 | 100% |
| Lorenz | 1.00 | — | 8.50 ± 0.01 | 0.20 ± 0.01 | 0.58 ± 0.02 | 0.91 ± 0.01 | 100% |
| | | W | 8.62 ± 0.05 | 1.33 ± 0.01 | 0.66 ± 0.03 | 0.76 ± 0.04 | 100% |

| System | $q$ | Noise | $S_{tot}$ | $D_{def}$ | $\nu$ | $\lambda_1$ | Survival |
|---|---|---|---|---|---|---|---|
| | | OU | 8.27 ± 0.10 | 0.62 ± 0.05 | 0.42 ± 0.03 | 0.64 ± 0.03 | 100% |
| | | SW | 8.67 ± 0.05 | 1.40 ± 0.01 | 0.65 ± 0.02 | 0.90 ± 0.04 | 100% |
| | | SOU | 8.30 ± 0.08 | 0.58 ± 0.03 | 0.44 ± 0.02 | 0.67 ± 0.04 | 100% |
| Chen | 0.85 | — | 6.69 ± 0.01 | 0.16 ± 0.00 | 1.88 ± 0.03 | 2.57 ± 0.02 | 100% |
| | | W | 7.93 ± 0.03 | 1.86 ± 0.02 | 5.12 ± 0.06 | 0.04 ± 0.02 | 100% |
| | | OU | 6.84 ± 0.02 | 0.38 ± 0.00 | 1.58 ± 0.05 | 1.66 ± 0.06 | 100% |
| | | SW | 7.99 ± 0.03 | 1.82 ± 0.03 | 4.55 ± 0.05 | 0.93 ± 0.09 | 100% |
| | | SOU | 6.82 ± 0.02 | 0.35 ± 0.01 | 1.70 ± 0.04 | 1.91 ± 0.04 | 100% |
| Chen | 0.99 | — | 6.94 ± 0.04 | 3.46 ± 1.52 | 2.39 ± 0.02 | 0.05 ± 0.07 | 100% |
| | | W | 9.25 ± 0.06 | 5.89 ± 0.08 | 4.60 ± 0.05 | 1.60 ± 0.06 | 100% |
| | | OU | 8.11 ± 0.04 | 5.02 ± 0.07 | 3.32 ± 0.03 | 1.96 ± 0.05 | 100% |
| | | SW | 10.07 ± 0.15 | 6.82 ± 0.14 | 4.74 ± 0.07 | 2.03 ± 0.06 | 96% |
| | | SOU | 8.00 ± 0.04 | 5.04 ± 0.08 | 3.23 ± 0.02 | 2.01 ± 0.05 | 100% |
| Chen | 1.00 | — | 8.13 ± 0.05 | 0.29 ± 0.01 | 3.41 ± 0.01 | 2.15 ± 0.02 | 100% |
| | | W | 9.51 ± 0.07 | 1.22 ± 0.03 | 4.78 ± 0.04 | 1.63 ± 0.06 | 100% |
| | | OU | 8.27 ± 0.06 | 0.53 ± 0.01 | 3.44 ± 0.03 | 1.89 ± 0.04 | 100% |
| | | SW | 10.88 ± 0.22 | 1.98 ± 0.13 | 5.03 ± 0.10 | 2.13 ± 0.06 | 83% |
| | | SOU | 8.15 ± 0.05 | 0.51 ± 0.01 | 3.37 ± 0.03 | 1.93 ± 0.05 | 100% |

Three results stand out in Table 3. First, at equal spectral intensity, white and state-dependent noise are far more effective than OU noise with $\tau = 0.5$ in every quantity. For Lorenz at $q = 0.99$ white noise at $\eta = 8$ restores a fully developed attractor ($S_{tot} = 8.51$, against 0.08 for the deterministic equilibrium) with $\lambda_1 = 0.72$, whereas OU noise gives $S_{tot} = 7.79$ with a smaller $\lambda_1$. Second, the state dependence has a smaller and more selective effect than the noise correlation. SW and W give similar dispersion and switching rates, but SW systematically leaves a larger exponent: in 43 of the 44 conditions in which the two differ significantly in $\lambda_1$ (of 71 compared) SW

gives the larger value (the single exception is Chen at $q = 0.80, \eta = 1$; for example Chen at $q = 0.85, \eta = 8$: 0.04 for W against 0.93 for SW). SW noise also limits survival: for Chen it cannot be used much above $\eta = 8$ because the multiplicative amplitude grows with $\| X \|$ and trajectories escape. Third, in the chaotic regime the largest exponent responds differently from the geometric quantities: the dispersion and switching rate increase with noise intensity while $\lambda_1$ decreases or stays near its deterministic value.

**Table 4.** Fraction of the (system, $q, \eta$) conditions in which two noise models differ significantly (Mann–Whitney test with Holm correction, adjusted $p < 0.05$); the number of conditions is in brackets.

| **Comparison** | $D_{def}$ | $H$ | $\nu$ | $\lambda_1$ |
|---|---|---|---|---|
| W vs OU (correlation) | 90% (71) | 70% (71) | 79% (71) | 83% (71) |
| W vs SW (state dependence, white) | 61% (71) | 39% (71) | 42% (71) | 62% (71) |
| OU vs SOU (state dependence, OU) | 42% (71) | 18% (71) | 32% (71) | 11% (71) |
| SW vs SOU | 90% (71) | 79% (71) | 82% (71) | 83% (71) |

Table 4 quantifies the ranking. Correlation matters in most conditions: white and OU noise differ significantly in the deformation in 90% of the conditions. State dependence matters in fewer: SW differs from W in 61% of the conditions for the deformation and 62% for $\lambda_1$, and SOU differs from OU in 42% and 11%. The correlation of the noise is therefore a stronger control variable than its state dependence, under the matched intensity conventions used here.

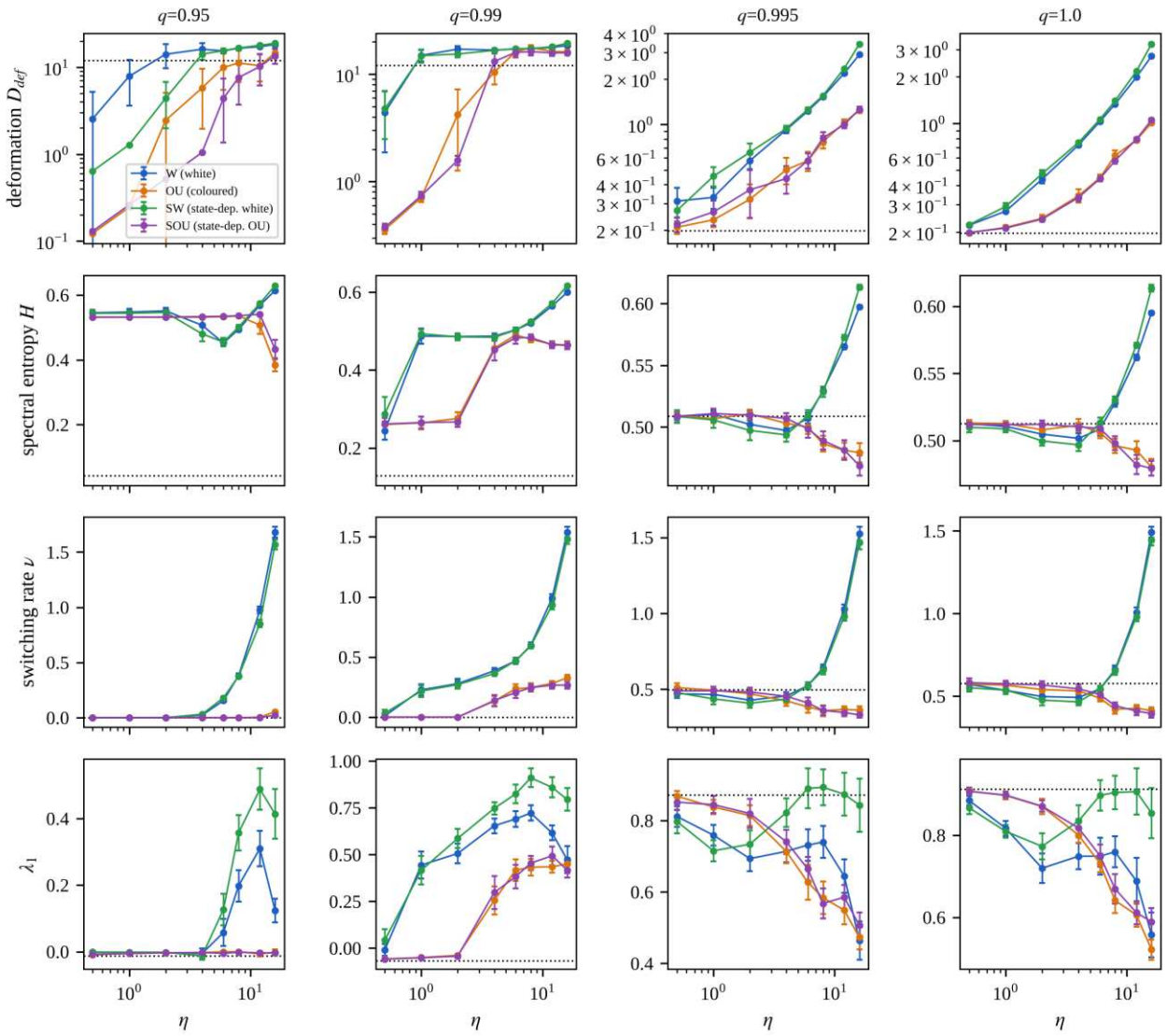



**Figure 7.** Response of the fractional Lorenz system to the four noise models against intensity $\eta$ ($\tau = 0.5$): deformation $D_{def}$, spectral entropy $H$, switching rate $\nu$ and tangent exponent $\lambda_1$ (rows) for each order $q$ (columns). Points: mean over realisations; bars: 95% confidence interval; dotted line: deterministic value.

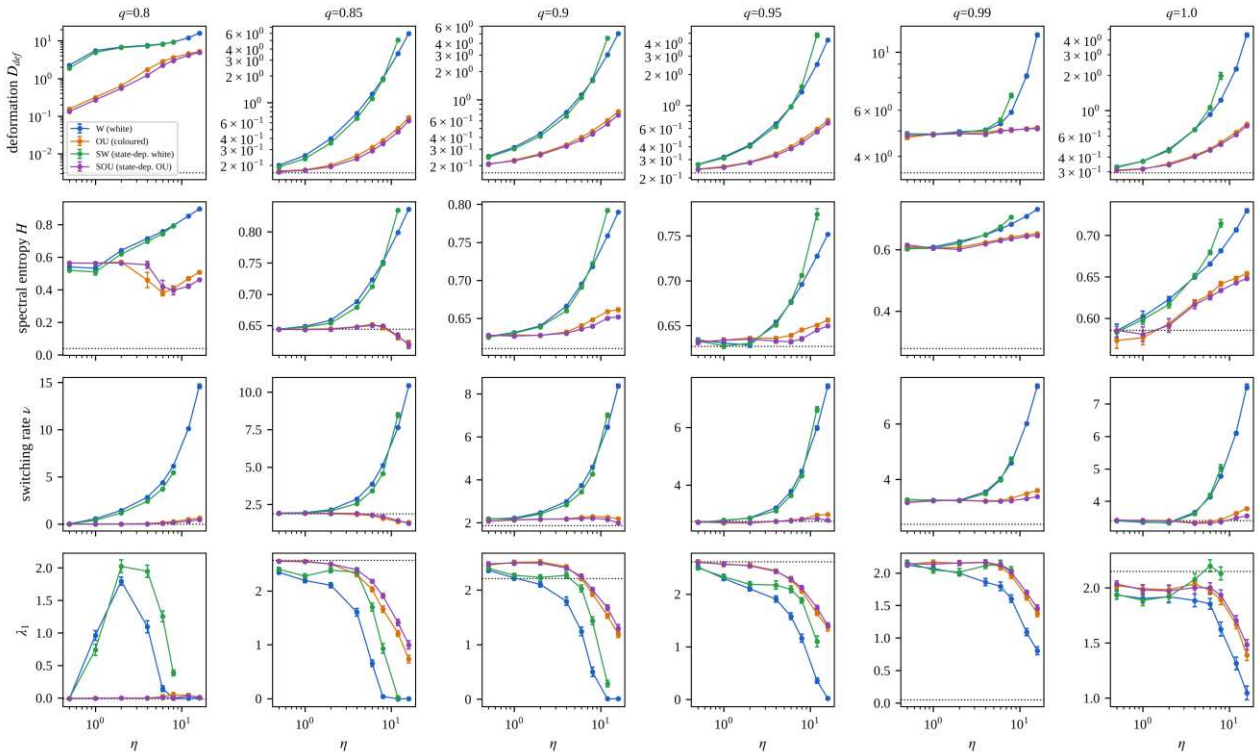



**Figure 8.** As Fig. 7 for the fractional Chen system. The curves for SW and SOU end where fewer than half of the runs remain bounded.

### Noise-Induced Order and Noise-Induced Chaos

**Table 5.** Smallest tested intensity $\eta$ (grid 0.5, 1, 2, 4, 6, 8, 12, 16) at which the mean exponent crosses 0.1 along the noise realisation. ">16" means that the criterion was not met in the tested range; for SW and SOU at large $\eta$ the criterion is evaluated on the surviving runs only.

| System | $q$ | Criterion | W | OU | SW | SOU |
|---|---|---|---|---|---|---|
| Lorenz | 0.95 | noise-sustained chaos ($\lambda_1 > 0.1$) | 8 | >16 | 6 | >16 |
| Lorenz | 0.99 | noise-sustained chaos ($\lambda_1 > 0.1$) | 1 | 4 | 1 | 4 |
| Chen | 0.99 | noise-induced chaos from a periodic window ($\lambda_1 > 0.1$) | 0.5 | 0.5 | 0.5 | 0.5 |
| Chen | 0.85 | noise-induced order ($\lambda_1 < 0.1$) | 8 | >16 | 12 | >16 |
| Chen | 0.90 | noise-induced order ($\lambda_1 < 0.1$) | 12 | >16 | >16 | >16 |
| Chen | 0.95 | noise-induced order ($\lambda_1 < 0.1$) | 16 | >16 | >16 | >16 |
| Chen | 1.00 | noise-induced order ($\lambda_1 < 0.1$) | >16 | >16 | >16 | >16 |

Table 5 summarises the two opposite effects of noise on the sign of $\lambda_1$. **Noise-induced order** occurs in the chaotic Chen system. White noise reduces $\lambda_1$ from about 2.6 to zero at $\eta = 8$ for $q = 0.85$, at $\eta = 12$ for $q = 0.9$ and at $\eta = 16$ for $q = 0.95$, while at $q = 1$ it only reaches $\lambda_1 = 1.05$ at $\eta = 16$. Nearby trajectories driven by the same white noise therefore converge, although the dispersion $S_{tot}$ and the switching rate $\nu$ have increased (for $q = 0.85$, $\nu$ rises from 1.9 to 5.1 at $\eta = 8$). The motion is strongly irregular but it is no longer sensitive to the initial condition, which is the

situation in which irregularity should not be called chaos. The critical intensity increases with $q$, so more memory (smaller $q$) makes the Chen system easier to order: this is the effect of fractional memory on noise-induced transitions asked about in the fourth research question. OU noise at equal spectral intensity and $\tau = 0.5$ does not reach the criterion, and SW does so only for $q = 0.85$ at $\eta = 12$, where just half of the runs remain bounded (Figs. 7 and 8).

**Noise-induced chaos** occurs in the opposite direction. In the equilibrium regime of the Lorenz system the deterministic exponent is neutral or negative ($-0.07$ at $q = 0.99$), but white noise at $\eta = 1$ produces $\lambda_1 = 0.44$, $S_{tot} = 7.3$ and a switching rate of 0.23 per time unit: a full-size attractor with a positive exponent is sustained by noise alone. At $q = 0.95$ the same state needs $\eta \approx 8$. Chen at $q = 0.99$ lies in a narrow periodic window ($\lambda_1 = 0.05$, $K = 0$); noise of the smallest tested intensity $\eta = 0.5$ raises $\lambda_1$ to about 2.1 and $S_{tot}$ from 6.9 to 7.9, so the window is destroyed by weak noise of any of the four types. This is consistent with the classical observation that noise can induce chaos (Gao et al., 1999). Because the state-dependent models and white noise sustain positive exponents in the equilibrium regime at similar intensities, the sign of the exponent along a noise realisation is a property of the combination of the vector field and the noise, not of the deterministic attractor.

**Correlation Time and Matching Convention**

Whether coloured noise looks stronger or weaker than white noise depends on how the two are matched, so the correlation time $\tau$ was swept from 0.05 to 5 at $\eta = 8$ under both conventions of Table 1 (Fig. 9). At **equal spectral intensity**, the OU forcing is a low-pass filtered version of white noise whose power at angular frequency $\omega$ is reduced by $1/(1 + \omega^2\tau^2)$, Equ. (10). The fractional Lorenz equilibrium at $q = 0.95$ oscillates near $\omega \approx 10$, where this factor is 0.04 at $\tau = 0.5$, and the response collapses: $S_{tot}$ falls from 7.97 at $\tau = 0.05$ (close to the white-noise value 8.15) to 1.31 at $\tau = 0.5$ and 0.24 at $\tau = 5$, and $\lambda_1$ falls from 0.14 to zero. For the chaotic Chen system at $q = 0.9$ the same increase of $\tau$ raises $\lambda_1$ from 0.81 to 2.55 (white noise: 0.50), that is, the order-inducing ability of the noise is lost as it becomes slower, and the deformation $D_{def}$ falls from 0.98 to 0.24. At **equal variance** the dependence on $\tau$ is weak for the chaotic systems ($S_{tot}$ of Chen at $q = 0.9$ stays between 7.04 and 7.17) because the forcing then carries comparable power in the band that matters, and for the Lorenz equilibrium the response is 1.69 at $\tau = 0.05$ and 0.78 at $\tau = 5$. The practical consequence is that a statement such as ‘coloured noise causes the largest deformation’, made in the original study without any matching convention, has no meaning on its own: in these data coloured noise is weaker than white noise under the equal-intensity rule at $\tau \geq 0.5$ and comparable to it under the equal-variance rule.

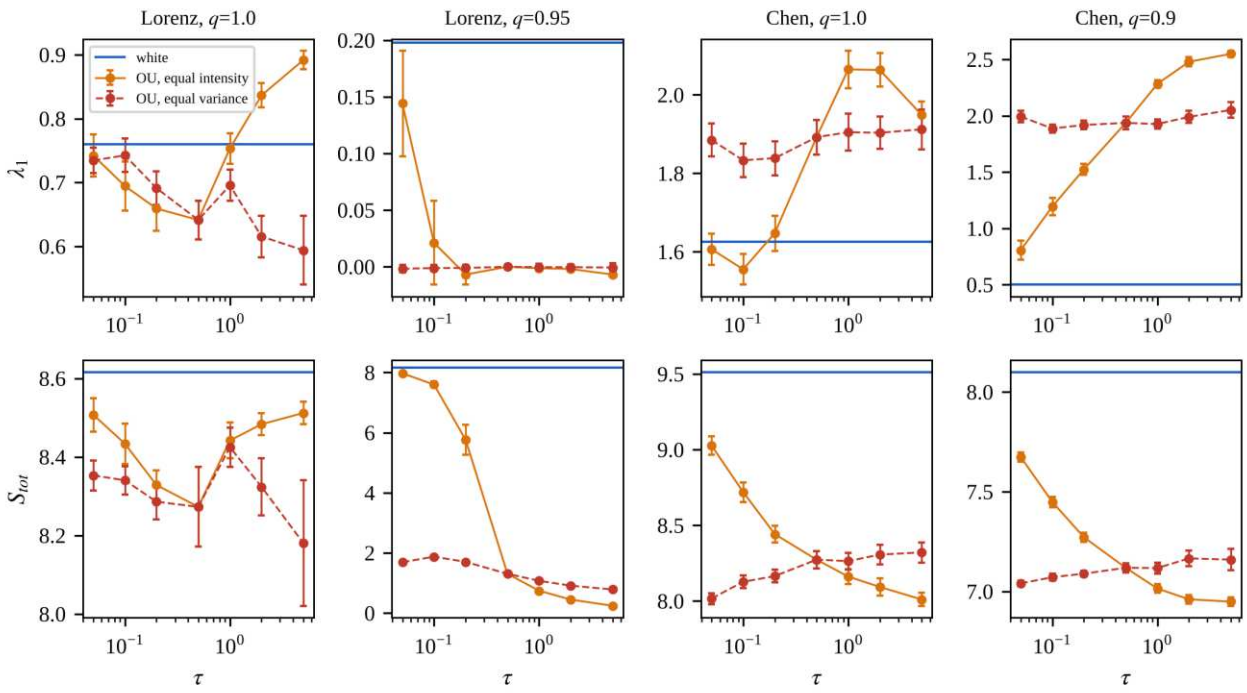



**Figure 9.** Effect of the correlation time $\tau$ of the OU noise at $\eta = 8$ under equal spectral intensity (solid) and equal variance (dashed): tangent exponent $\lambda_1$ (top) and dispersion $S_{tot}$ (bottom), with 95% confidence intervals. The horizontal line is the white-noise value.

### Independent Check of the Exponent with Twin Trajectories

**Table 6.** Tangent exponent compared with the growth rate of the separation of twin trajectories started $10^{-8}$ apart and driven by the same noise (16 realisations, slope of the mean of $\ln \| \Delta X \|$ between $10^{-8}$ and $e^{-3}$). "Decays to round-off" means that the separation shrinks and no growth phase exists.

| System | $q$ | Noise | $\eta$ | $\lambda_1$ (tangent) | Twin slope |
|---|---|---|---|---|---|
| Lorenz | 1.00 | — | 0 | 0.83 | 0.55 |
| Lorenz | 1.00 | W | 8 | 0.79 | 0.73 |
| Lorenz | 1.00 | OU | 8 | 0.59 | 0.63 |
| Lorenz | 1.00 | SW | 8 | 0.94 | 0.90 |
| Lorenz | 0.95 | W | 8 | 0.21 | 0.15 |
| Lorenz | 0.95 | W | 20 | 0.00 | decays to round-off |
| Chen | 1.00 | — | 0 | 2.34 | 1.93 |
| Chen | 1.00 | W | 8 | 1.54 | 1.69 |
| Chen | 1.00 | OU | 8 | 1.86 | 1.85 |
| Chen | 1.00 | SW | 8 | 1.98 | 2.16 |
| Chen | 0.90 | W | 20 | -0.01 | decays to round-off |
| Chen | 0.90 | OU | 20 | 0.84 | 0.60 |

The two estimates agree on the sign and on the ordering in every case (Table 6, Fig. 10). The twin slope is systematically smaller than the tangent exponent for the deterministic and weakly forced systems (for example 1.93 against 2.34 for Chen at $q = 1$) because it is fitted over a finite window that also contains the initial transient

of the perturbation direction and, for $q < 1$, the memory of the common history; the tangent value is the better estimate of the asymptotic rate, the twin run is the check that the sign is not an artefact of the tangent equation. For strong noise the two agree that the separation is not amplified: at $q = 0.95, \eta = 20$ and at Chen $q = 0.9, \eta = 20$ the separation of the twins decays to round-off, which is noise-induced synchronisation of trajectories driven by a common noise record.

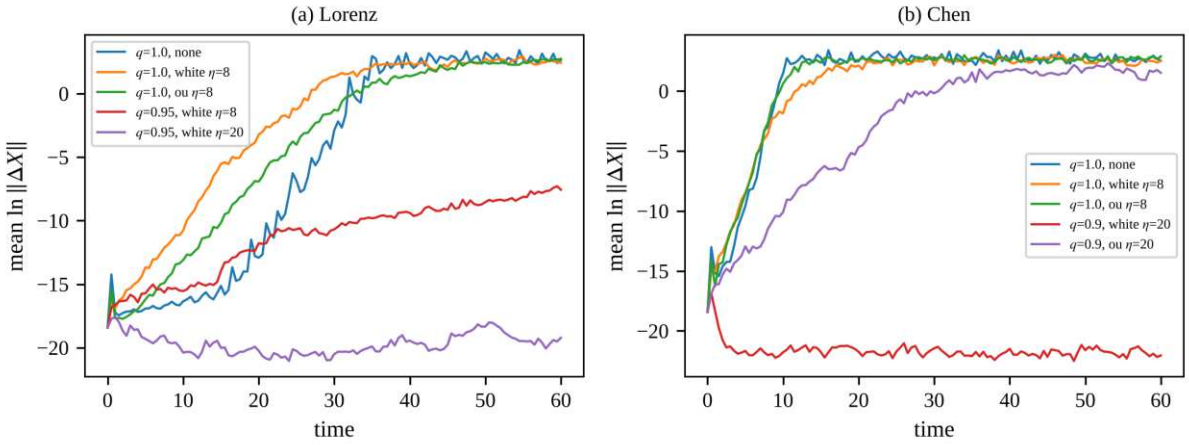



**Figure 10.** Mean logarithmic separation of twin trajectories started $10^{-8}$ apart and driven by the same noise record. (a) Lorenz. (b) Chen. Growth followed by saturation indicates sensitivity to initial conditions; a decreasing curve indicates convergence of trajectories driven by common noise.

**Robustness against the Time Step**

**Table 7.** Step-size test with common random numbers (16 realisations). "Unstable" means that fewer than half of the runs stayed bounded.

| **System** | $q$ | **Noise** | $\eta$ | $S_{tot}, h = 0.02$ | **0.01** | **0.005** | $\lambda_1, h = 0.02$ | **0.01** | **0.005** |
|---|---|---|---|---|---|---|---|---|---|
| Lorenz | 1.00 | W | 8 | 8.61 | 8.64 | 8.64 | 0.71 | 0.77 | 0.77 |
| Lorenz | 0.95 | W | 8 | 8.19 | 8.20 | 8.19 | 0.28 | 0.28 | 0.27 |
| Chen | 1.00 | W | 4 | unstable | 8.36 | 8.28 | unstable | 1.89 | 1.79 |
| Chen | 0.90 | W | 4 | 7.67 | 7.31 | 7.25 | 2.30 | 1.84 | 1.75 |
| Chen | 0.90 | W | 8 | unstable | 8.12 | 8.04 | unstable | 0.48 | 0.37 |
| Chen | 0.90 | OU | 8 | unstable | 7.08 | 7.02 | unstable | 1.95 | 1.77 |

The dispersion changes by less than 2% between $h = 0.01$ and $h = 0.005$ in every case of Table 7. The tangent exponent is more demanding: it is converged to within about 0.02 for the Lorenz system and to within 0.1–0.2 for the Chen system, and for Chen at $q = 0.9$ with white noise at $\eta = 8$, close to the point where $\lambda_1$ crosses zero, it moves from 0.48 to 0.37 when the step is halved. The qualitative result, a decrease of $\lambda_1$ with intensity that is stronger for smaller $q$, is unchanged, but the intensity at

which the criterion of Table 5 is met should be read as accurate to about one grid step. At $h = 0.02$ the Chen system with strong noise is numerically unstable, which is the reason why the production runs use $h = 0.01$ and the sensitive cases were checked at 0.005.

**Why Per-Step Additive Noise Is Not a Valid Fractional Noise Model**

The update of the original study, $x_{n+1} = x_n + h^\alpha F(x_n) + \xi_n$, has two defects that the present analysis makes explicit. First, it contains no memory: it is the explicit Euler method with the effective step $h^\alpha$, so $\alpha$ only rescales the time step ($0.01^{0.85} = 0.020$) and no history is stored. Integrated deterministically with $h = 0.01$, this update keeps the Lorenz system chaotic at $\alpha = 0.85$ (standard deviations of $x, y, z$: 8.5, 9.7, 8.4) and at $\alpha = 0.95$ (8.3, 9.3, 7.9), whereas the Caputo system of Equ. (2) relaxes to an equilibrium for all $q \leq 0.99$ (Table 2). Statements about the chaotic behaviour of the fractional Lorenz system based on that update are therefore not statements about the fractional system. Second, adding a random number of fixed standard deviation $d$ at every step is not a discretisation of any continuous noise: the injected variance per unit time is $d^2/h$ and diverges as $h \to 0$. In the linear test the stationary variance of the per-step form rises from 3.19 to 25.06 when $h$ is reduced from 0.04 to 0.005, whereas the scaled form $d\sqrt{h}\,N(0,1)$ gives the constant 0.128 (Fig. 11a). The chaotic dispersion hides this defect, because it saturates at the attractor size (Fig. 11b), which is why it is easy to overlook. Third, the construction of the 'state-dependent' term does not deliver what its name states: with independent uniform arguments the Box–Muller expression is Gaussian noise (Kolmogorov–Smirnov $D = 0.0024$, $p = 0.20$; skewness -0.00, excess kurtosis 0.01), indistinguishable from the Gaussian noise of the first model, so the three-way comparison of the original study was effectively a two-way comparison with an undefined second element.

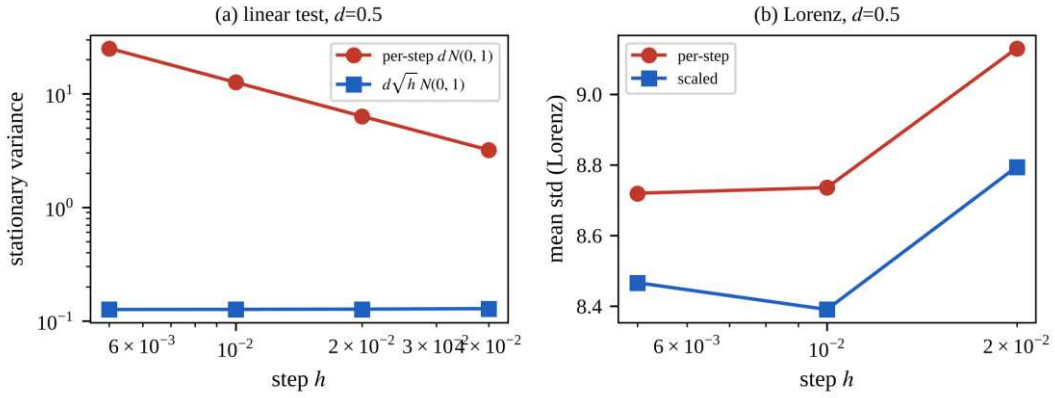



**Figure 11.** Failure of per-step additive noise. (a) Stationary variance of a linear test system as a function of the step $h$, for the per-step form $d\,N(0,1)$ and the scaled form $d\sqrt{h}\,N(0,1)$ ($d = 0.5$). (b) Mean standard deviation of the Lorenz state, which is nearly unchanged because it saturates at the attractor size.

**Discussion**

**Memory sets the stage and noise decides what happens on it.** The chaos boundary of Equ. (6) separates two physically different problems. Below it the equilibria are stable, so every irregular signal is produced by the noise. The response is then a linear-response problem for weak noise, as the quantitative agreement in Fig. 3 shows, and a nonlinear one once the excursions reach the size of the old attractor (the departure of the white-noise points at $\eta \gtrsim 2$). Above the boundary the attractor exists

and noise modifies it. The fractional Lorenz system lies only 0.4% below its boundary at $q = 0.99$, so a small amount of noise suffices to rebuild a full-size attractor with a positive exponent, which is what the earlier literature calls noise-induced chaos (Gao et al., 1999). The Chen system has more room, and in it the opposite effect appears: strong white noise reduces the exponent to zero, the noise-induced order of Matsumoto and Tsuda (1983), here accompanied by a larger dispersion and a larger switching rate. These two outcomes are not contradictory; they are the same mechanism, the response of the exponent along a noise realisation, on opposite sides of the sign change.

**Order versus irregularity.** The time series of the ordered Chen runs are more irregular than the deterministic ones and look chaotic, yet nearby trajectories driven by the same noise converge. A study based on phase portraits and time series alone would classify these runs as chaotic. This is the strongest argument for using the exponent along the noise record, together with the geometric and spectral measures, instead of the visual statements used in the original manuscript.

**Correlation is a stronger control variable than state dependence, and the ranking is convention dependent.** At equal spectral intensity white noise is stronger than OU noise with $\tau \geq 0.5$ because the fractional systems respond at frequencies of order 10, where the OU spectrum is small. At equal variance the two are comparable. Any ranking of 'white versus coloured' noise therefore needs its matching rule stated, which the original conclusion did not do. The state-dependent modulation changes the geometric quantities in most conditions, but it matters less for the exponent when the noise is coloured (it differs significantly in only 11% of the conditions for OU against SOU, against 62% for W against SW). Where it matters, it increases $\lambda_1$ (43 of 44 significant cases) and reduces survival, because the amplitude grows with $\| X \|$ and positive feedback between excursion and amplitude can escape to infinity.

Relating to previous research, Adelakun et al. (2019) obtained chaos suppression from a term that depends on the states $x$ and $y$ through the Box–Muller expression. Because there is no random input, that term is a nonlinear feedback that changes the vector field, and suppression by it is a control effect and not a noise effect. The present study treats genuinely stochastic forcing and shows that suppression of the sensitivity to initial conditions requires sufficiently strong white noise and is stronger when the memory is larger, whereas weak noise does not suppress chaos in either system. The use of a validated threshold-based classification, step-size sensitivity and an independent check of the exponent follows the protocol of Ajayi (2026), and the deterministic-memory perspective of that memcapacitor study is here replaced by the fractional memory kernel.

## Limitations of the Research

The exponent defined by Equ. (18) is a finite-time, tangent-equation exponent for a system with memory; it has no semigroup structure and, in the stable regime, decays algebraically, so values near zero are classified with a neutral band and not by sign alone. The runs cover 150 time units with 24 realisations per condition, which gives confidence intervals of a few per cent for the dispersion but wider ones for the exponent near its sign change. The intensity grid is coarse (factor of two), and the critical intensities of Table 5 are accurate to one grid step and to the step-size effect discussed above. One parameter set per system and one correlation time ($\tau = 0.5$) are used in the main grid, and the amplitude modulation $g(X) = \| X \| / R_N$ is one choice

among many. Noise sources are independent across components and the stochastic integrals are of Itô type. These choices define the scope of the conclusions.

## CONCLUSION

The effect of Gaussian, coloured and state-dependent noise on the Caputo fractional-order Lorenz and Chen systems was compared with a verified stochastic Adams–Bashforth–Moulton scheme in which the noise enters through the memory kernel. The scheme reproduces the exact Mittag-Leffler solution with the theoretical order, the exact variance of the stochastic Volterra integral to within 1.3%, and the linear-response prediction of the equilibrium fluctuations. The chaos boundary of the memory, $q_L^* = 0.994$ and $q_C^* = 0.824$, organises the results. The fractional Lorenz system with the classical parameters is not chaotic for $q \leq 0.99$, which invalidates conclusions drawn at those orders from memory-less updates. Below the boundary, noise creates irregular motion whose size follows the linear-response theory for weak noise, and white noise of modest intensity sustains an attractor with a positive exponent ($\lambda_1 = 0.44$ at $q = 0.99, \eta = 1$). Above the boundary, in the Chen system, noise has the opposite effect on the sign of the exponent: white noise reduces $\lambda_1$ from about 2.6 to zero at $\eta = 8$ ($q = 0.85$), $\eta = 12$ ($q = 0.9$) and $\eta = 16$ ($q = 0.95$), so more memory makes noise-induced order easier, while the dispersion and the switching rate increase. At $q = 1$ it does not reach zero in the tested range. Gaussian noise sustains chaos below the boundary and removes sensitivity above it in Chen, depending on intensity. State-dependent amplitude has a smaller effect than correlation, increases the exponent relative to additive noise in nearly all significant cases and limits survival. The most effective noise for removing chaos is white noise; OU noise with $\tau = 0.5$ at equal spectral intensity is much weaker, and the ranking depends on the matching rule. Memory, measured by the distance of $q$ from the boundary, lowers the intensity needed for noise-induced order and raises the sensitivity of the Lorenz system to noise-induced chaos. Per-step additive noise has no continuum limit, the Box–Muller expression with random arguments is Gaussian noise, and statements about chaos suppression need a quantitative criterion such as the exponent along the noise record. The conclusions are limited to the parameter sets, grid and noise definitions given above. Direct applications, for example to secure communication or chaos control, were not evaluated here and remain topics for future work, together with the deterministic feedback noise of Adelakun et al. (2019), other fractional-order systems, incommensurate orders and hardware realisations of memory elements.

## DECLARATIONS

**Funding:** The research received no specific grant from any funding agency.

**Clinical Trial Registration:** This research does not involve a clinical trial.

**Ethics Approval:** Not applicable.

**Competing Interest:** The authors declare that there is no competing interest regarding this research.

**Author Contribution:** I. O. Ajayi conceived the study, designed the computational framework, carried out the numerical simulations, analysed and interpreted the results, prepared the figures and wrote the manuscript. T. A. Ojuola Validation, Supervision and Proof reading. O. S. Adeosun contributed to the conceptualisation,

supervision and revision of the manuscript. All authors approved the final version. S. A. Olawoore contributed writeup, validation and Proof reading.

**Code Availability:** The C solver and Python scripts used for the simulations and figures are available from the corresponding author upon reasonable request.

**Data Availability:** The datasets generated and analysed during this research are available from the corresponding author upon reasonable request.

**Consent to Publish:** Not applicable.

**Consent to Participate:** Not applicable.

## REFERENCES


Adelakun, A. O., Egunjobi, A. I., & Adeyeri, J. A. (2026). Hyperchaos in a series-connected memcapacitor system. *Discover Electronics*, 3(1), 85. https://doi.org/10.1007/s44291-026-00236-5

Adelakun, A. O., Ogunjo, S. T., & Fuwape, I. A. (2019). Chaos suppression in fractional order systems using state-dependent noise. *SN Applied Sciences*, 1(12), 1608. https://doi.org/10.1007/s42452-019-1599-5

Ahmad, W. M., & Sprott, J. C. (2003). Chaos in fractional-order autonomous nonlinear systems. *Chaos, Solitons & Fractals*, 16(2), 339–351.

Ajayi, I. O. (2026). Chaotic dynamics, basin structure and global dynamical analysis of a six-dimensional series memcapacitor system. [Journal, volume, pages and DOI to be inserted by the author before submission].

Almutairi, N., & Saber, S. (2024). Existence of chaos and the approximate solution of the Lorenz–Lü–Chen system with the Caputo fractional operator. *AIP Advances*, 14(1), 015112. https://doi.org/10.1063/5.0185906

Arnold, L. (1998). *Random Dynamical Systems*. Springer, Berlin.

Chen, G., & Ueta, T. (1999). Yet another chaotic attractor. *International Journal of Bifurcation and Chaos*, 9(7), 1465–1466.

Crutchfield, J. P., Farmer, J. D., & Huberman, B. A. (1982). Fluctuations and simple chaotic dynamics. *Physics Reports*, 92(2), 45–82.

Danca, M.-F., & Kuznetsov, N. (2018). Matlab code for Lyapunov exponents of fractional-order systems. *International Journal of Bifurcation and Chaos*, 28(5), 1850067.

Das, S., Pan, I., & Das, S. (2016). Effect of random parameter switching on commensurate fractional order chaotic systems. *Chaos, Solitons & Fractals*, 91, 157–173.

Diethelm, K., Ford, N. J., & Freed, A. D. (2002). A predictor-corrector approach for the numerical solution of fractional differential equations. *Nonlinear Dynamics*, 29, 3–22.

Diethelm, K., Ford, N. J., & Freed, A. D. (2004). Detailed error analysis for a fractional Adams method. *Numerical Algorithms*, 36(1), 31–52.

Doan, T. S., Huong, P. T., Kloeden, P. E., & Vu, A. M. (2020). Euler–Maruyama scheme for Caputo stochastic fractional differential equations. *Journal of Computational and Applied Mathematics*, 380, 112989. https://doi.org/10.1016/j.cam.2020.112989

Gao, J. B., Hwang, S. K., & Liu, J. M. (1999). When can noise induce chaos? *Physical Review Letters*, 82(6), 1132–1135.

Gottwald, G. A., & Melbourne, I. (2004). A new test for chaos in deterministic systems. *Proceedings of the Royal Society A*, 460, 603–611.

Gottwald, G. A., & Melbourne, I. (2005). Testing for chaos in deterministic systems with noise. *Physica D*, 212, 100–110.

Gottwald, G. A., & Melbourne, I. (2009). On the implementation of the 0–1 test for chaos. *SIAM Journal on Applied Dynamical Systems*, 8(1), 129–145.

Grigorenko, I., & Grigorenko, E. (2003). Chaotic dynamics of the fractional Lorenz system. *Physical Review Letters*, 91(3), 034101. https://doi.org/10.1103/PhysRevLett.91.034101

Hänggi, P., & Jung, P. (1995). Colored noise in dynamical systems. *Advances in Chemical Physics*, 89, 239–326.

He, S., Banerjee, S., & Sun, K. (2018). Can derivative determine the dynamics of fractional-order chaotic system? *Chaos, Solitons & Fractals*, 115, 14–22. https://doi.org/10.1016/j.chaos.2018.08.013

Holm, S. (1979). A simple sequentially rejective multiple test procedure. *Scandinavian Journal of Statistics*, 6(2), 65–70.

Kilbas, A. A., Srivastava, H. M., & Trujillo, J. J. (2006). *Theory and Applications of Fractional Differential Equations*. Elsevier, Amsterdam.

Li, C., & Peng, G. (2004). Chaos in Chen's system with a fractional order. *Chaos, Solitons & Fractals*, 22(2), 443–450.

Lorenz, E. N. (1963). Deterministic nonperiodic flow. *Journal of the Atmospheric Sciences*, 20(2), 130–141.

Lu, J. G., & Chen, G. (2006). A note on the fractional-order Chen system. *Chaos, Solitons & Fractals*, 27(3), 685–688. https://doi.org/10.1016/j.chaos.2005.04.037

Matignon, D. (1996). Stability results for fractional differential equations with applications to control processing. In *Computational Engineering in Systems Applications* (Vol. 2, pp. 963–968). IMACS/IEEE-SMC, Lille.

Matsumoto, K., & Tsuda, I. (1983). Noise-induced order. *Journal of Statistical Physics*, 31(1), 87–106.

Podlubny, I. (1999). *Fractional Differential Equations*. Academic Press, San Diego.

Tavazoei, M. S., & Haeri, M. (2007). A necessary condition for double scroll attractor existence in fractional-order systems. *Physics Letters A*, 367(1–2), 102–113.

Thounaojam, U. S. (2022). Stochastic chaos in chemical Lorenz system: Interplay of intrinsic noise and nonlinearity. *Chaos, Solitons & Fractals*, 165, 112763. https://doi.org/10.1016/j.chaos.2022.112763

Uhlenbeck, G. E., & Ornstein, L. S. (1930). On the theory of the Brownian motion. *Physical Review*, 36, 823–841.

Welch, P. D. (1967). The use of fast Fourier transform for the estimation of power spectra. *IEEE Transactions on Audio and Electroacoustics*, 15(2), 70–73.

Zhang, X. (2008). Euler schemes and large deviations for stochastic Volterra equations with singular kernels. *Journal of Differential Equations*, 244(9), 2226–2250.

Zhou, C., & Kurths, J. (2002). Noise-induced phase synchronization and synchronization transitions in chaotic oscillators. *Physical Review Letters*, 88, 230602.